Highlights

Multifractal Detrended Cross-Correlation Coefficient for Cosmic Ray and Sunspot Time Series

D. Sierra-Porta

- Significant multifractal correlations between cosmic rays and sunspots are revealed.
- The ability of MFDCCA to capture complex dependencies across scales is highlighted.
- Improved space weather models based on multifractal analysis are proposed.

Multifractal Detrended Cross-Correlation Coefficient for Cosmic Ray and Sunspot Time Series

D. Sierra-Porta[a,1]

[a] *Universidad Tecnológica de Bolívar, UTB. Facultad de Ciencias Básicas., Parque Industrial y Tecnológico Carlos Vélez Pombo Km 1 Vía Turbaco., Cartagena de Indias, 130010, Bolívar, Colombia*

Abstract

This study delves into the multifractal cross-correlations between cosmic ray intensity and sunspot numbers, addressing the shortcomings of traditional correlation analyses that often fail to capture the intricate and multifractal nature of these time series. Cosmic rays and solar activity are critical components of space weather dynamics, and understanding their interactions is essential for predicting space weather events that can affect satellite operations, communication systems, and even climate on Earth. We employ Multifractal Detrended Cross-Correlation Analysis (MFDCCA) to explore these complex relationships across a range of time scales. Our methodology involves segmenting the time series into windows of varying lengths, from 50 to 3900 days, and calculating cross-correlation coefficients for different polynomial fitting orders and fluctuation orders $q = [0.5, 1, 2, 3, 4, 5]$, using polynomial orders of 2, 3, 4, and 5. This approach allows us to capture the multifractal properties and temporal dependencies within and between the series.

Our analysis reveals significant multifractal correlations, with the highest correlation coefficient of 0.876 occurring for $q = 0.5$ and polynomial order 2 with a lag of 57 days. The results demonstrate that higher polynomial orders result in more stable and robust coefficients, indicating stronger correlations on larger scales. These findings highlight the efficacy of advanced techniques like MFDCCA in uncovering the complex interactions between cosmic rays and solar activity, which are often missed by conventional methods. The implications of our study extend to the enhancement of space weather prediction models. By incorporating additional heliophysical variables such as solar wind conditions, interplanetary magnetic field data, and indices of coronal mass ejections or solar flares, future research can construct more comprehensive models that better capture the multifractal interactions governing these phenomena. This expanded understanding is crucial for improving the accuracy of space weather forecasts and mitigating the potential impacts of space weather events on technological and natural systems.

Keywords: Multifractal Detrended Cross-Correlation Analysis, Cosmic Ray Intensity, Sunspot Numbers, Time Lag Analysis, Space Weather Dynamics

1. Introduction

In various complex systems, the interactions between components can be highly intricate, with the current value of each component depending not only on its own past but also on the past values of other components. This complexity is particularly evident in non-stationary systems that exhibit long-range correlations and cross-correlations [1, 2, 3]. Traditional correlation analysis methodologies, such as covariance analysis, often fall short in capturing these dynamics due to their inability to address non-stationary behavior effectively.

Detrended cross-correlation analysis (DCCA) [4, 5] and the recently explored detrended cross-correlation coefficient (ρ_{DCCA}) [6, 7, 8] have been proposed to address this limitation, providing tools to quantify the significance of cross-correlations in non-stationary time series. These methodologies have revealed complex patterns across various fields, including geophysics, economics, and material physics. For example, studies of the Chinese financial market

Email address: dporta@utb.edu.co (D. Sierra-Porta)
[1] Corresponding author

have shown a weak cross-correlation with the U.S. market, highlighting the relative independence of the Chinese market from external influences [9, 10]. Similarly, research in the cryptocurrency market has quantified its complexity from different perspectives [11, 12]. Other areas of application include the characterization of weather systems, global climate, and transient phenomena such as the North Atlantic Oscillation [13, 14, 15], as well as the analysis of atmospheric pollutants in urban areas [16, 17]. Additionally, in the context of space weather, cosmic rays have also been related to various phenomena and factors associated with terrestrial climate and meteorological variables [18, 19].

Multifractality has emerged as a critical feature in the study of time series in astrophysics and other natural sciences [20, 21, 22, 23, 24]. The ability of multifractal methods to describe fluctuations across multiple time scales offers deeper insights into the underlying processes that generate these series. Previous studies have applied multifractal analysis to unravel the multifaceted interactions and variability of cosmic rays and their relationship with solar activity [25]. These studies have demonstrated that multifractal characteristics are crucial for a more detailed understanding of astrophysical phenomena, including the identification of patterns and the prediction of solar events.

Sunspot time series are generally non-stationary due to long-term trends, significant cyclical variations such as the approximately 11-year solar cycle, and changes in variance over time. Similarly, cosmic ray time series recorded by neutron monitors on Earth are also non-stationary, influenced by factors including solar activity, geomagnetic conditions, and atmospheric effects, leading to long-term trends and variability in the data. These characteristics make traditional correlation measures less effective for capturing the complex dynamics present.

Several studies have employed DCCA, which is based on Detrended Fluctuation Analysis (DFA), to investigate the cross-correlations between non-stationary time series. DFA is a widely used method for detecting long-range correlations by detrending the data over various scales and analyzing the resulting fluctuation functions. DCCA extends DFA by applying it to pairs of time series, enabling the study of cross-correlations at multiple scales.

In recent years, several studies have focused on measuring the time lag between cosmic rays and sunspot numbers using various correlation techniques [26, 27, 28]. For instance, Koldobskiy et al. [29] utilized cross-correlation functions to examine the time delay between solar activity and galactic cosmic ray intensity, finding a notable lag that varies with solar cycles. Similarly, Idosa et al. [30] applied wavelet analysis and cross-correlation methods to identify the temporal relationships between cosmic ray flux and solar activity indicators, highlighting significant lags and periodicities.

Recent work by Modzelewska et al. [31] and Sierra-Porta and Domínguez-Monterroza [23] explored the use of DCCA to analyze the scaling properties of the diurnal variation of galactic cosmic rays during Solar Cycle 24 and the solar minima between Solar Cycles 23/24 and 24/25 based on neutron monitor count rates. The scaling features of the galactic cosmic ray diurnal variation are studied by evaluating the Hurst exponent, a quantitative parameter used as an indicator of the state of randomness in a time series.

In this study, we extend the traditional DCCA approach by generalizing it to use Multifractal Detrended Fluctuation Analysis (MFDFA) to provide a more robust framework for studying correlations between solar dynamics and cosmic ray count time series. Although DFA and DCCA typically assume monofractality [13], where a single scaling exponent characterizes the time series, MFDFA allows the detection of multifractality, capturing a spectrum of scaling exponents that describe the complexity of the data more comprehensively [32]. This multifractal approach is particularly advantageous for characterizing the intricate and heterogeneous scaling behaviors often observed in natural systems, such as the variability in cosmic rays and sunspot numbers.

The objective of this manuscript is to use a version of the correlation coefficient that employs multifractal characteristics of the involved time series, quantifying the significance of these correlations more generally. By combining the methodologies of DCCA with multifractal analysis, we aim to provide a robust tool for evaluating cross-correlations in complex and non-stationary time series. This approach will not only enhance our understanding of the relationships between cosmic rays and sunspots but also have broader applications in other fields of science and engineering.

2. Methods and Data Experiment

2.1. Multifractal Detrended Cross-Correlation Coefficient

In the analysis of stationary time series, cross-covariance and cross-correlation functions are commonly employed to quantify the similarity between two series [33, 34]. These measures also help assess the statistical significance of

cross-correlations. However, when dealing with non-stationary time series, these traditional measures are inadequate as they do not account for non-stationarity in the data. To address this issue, MFDCCA and the multifractal detrended cross-correlation coefficient ρ_{MFDCCA} [7, 8] have been developed.

To define the multifractal detrended cross-correlation coefficient for two non-stationary time series x_i and y_i of equal length N, we begin by computing their integrated signals [4, 9]:

$$X_k = \sum_{i=1}^{k} x_i \quad \text{and} \quad Y_k = \sum_{i=1}^{k} y_i, \tag{1}$$

where $k = 1, \ldots, N$.

The integrated series are then divided into overlapping windows of length n. Within each window, a local polynomial trend is fitted to the data, and the detrended series are obtained by subtracting this local trend from the integrated series. The detrended covariance for each window, starting at index i and ending at $i + n$, is calculated as:

$$f^2_{\text{MFDCCA},xy}(n, i) = \frac{1}{n} \sum_{k=i}^{i+n} \left[(X_k - \tilde{X}_{k,i})(Y_k - \tilde{Y}_{k,i}) \right]^q, \tag{2}$$

where $\tilde{X}_{k,i}$ and $\tilde{Y}_{k,i}$ are the local polynomial trends in the window, and q is the multifractal order.

In the context of MFDCCA, the parameter q represents the order of the statistical moments analyzed. It allows for the examination of the scaling behavior of fluctuations of different magnitudes within the time series. Positive values of q emphasize larger fluctuations, while negative values highlight smaller fluctuations [35, 36]. This parameter provides a deeper understanding of the multifractal structure of the time series by revealing how different scales of variability contribute to the overall dynamics.

The overall detrended covariance $F_{\text{MFDCCA}}(n, q)$ is obtained by averaging over all windows:

$$F^2_{\text{MFDCCA},xy}(n, q) = \left[\frac{1}{N - n} \sum_{i=1}^{N-n} f^2_{\text{MFDCCA},xy}(n, i) \right]^{1/q}. \tag{3}$$

The multifractal detrended variance is calculated similarly for each series. For the series x_i, it is given by:

$$F^2_{\text{MFDFA},x}(n, q) = \left[\frac{1}{N - n} \sum_{i=1}^{N-n} \left[(X_k - \tilde{X}_{k,i})^2 \right]^q \right]^{1/q}. \tag{4}$$

Analogously, for the series y_i:

$$F^2_{\text{MFDFA},y}(n, q) = \left[\frac{1}{N - n} \sum_{i=1}^{N-n} \left[(Y_k - \tilde{Y}_{k,i})^2 \right]^q \right]^{1/q}. \tag{5}$$

Understanding the scaling properties of $F^2(n, q)$ is crucial for deciphering the multifractal behavior of time series. For a given window size n, the fluctuation function $F^2(n)$ scales with n following a power-law relationship, $F^2(n) \propto n^{2H}$, where H is the Hurst exponent. The Hurst exponent characterizes the long-term memory of the time series: $0 < H < 0.5$ indicates anti-persistent behavior, $H = 0.5$ corresponds to a random walk, and $0.5 < H < 1$ signifies persistent behavior. This relationship allows us to quantify the degree of long-range dependence in the data.

The multifractal detrended cross-correlation coefficient $\rho_{\text{MFDCCA}}(n, q)$ is then defined as the ratio of the multifractal detrended covariance to the geometric mean of the multifractal detrended variances [7, 8]:

$$\rho_{\text{MFDCCA}}(n, q) = \frac{F^2_{\text{MFDCCA},xy}(n, q)}{F_{\text{MFDFA},x}(n, q) \cdot F_{\text{MFDFA},y}(n, q)}. \tag{6}$$

The coefficient $\rho_{\text{MFDCCA}}(n, q)$ used in this study ranges between 0 and 1, as the calculation involves adding fluctuations without retaining their signs. A value close to 1 indicates strong cross-correlations, while values near 0 suggest

no significant cross-correlations. This approach focuses on the magnitude of the correlation, consistent with the method employed here. The significance of $\rho_{\mathrm{MFDCCA}}(n, q)$ can be further tested using statistical methods to determine the presence of genuine cross-correlations between the two time series.

Future studies may consider implementing the modified definition of the multifractal detrended cross-correlation coefficient to include the sign of the fluctuations, thereby obtaining values in the range [-1, 1]. However, as the negative correlation between cosmic ray intensity and sunspot numbers is well known, the present analysis focuses on quantifying the magnitude of the correlation, which remains meaningful for understanding the multifractal relationship between these two time series.

Using the MFDCCA coefficient, we can capture the multifractal nature of the data and quantify the significance of cross-correlations with greater accuracy. This approach provides a more comprehensive understanding of the relationships between complex and non-stationary time series.

2.2. Test Data

The cosmic ray data utilized in this study were obtained from the Neutron Monitor Data Base (NMDB, `https://www.nmdb.eu/`) [37, 38, 39], specifically from the OULU station. The NMDB provides a comprehensive collection of cosmic ray measurements from various neutron monitor stations worldwide, offering valuable insights into cosmic ray intensity and its variations over time.

The OULU neutron monitor station is located at 65.05° N, 25.47° E, at an altitude of 15 meters above sea level. It has a magnetic rigidity cutoff of approximately 0.8 GV, enabling it to measure lower-energy cosmic rays that are more strongly influenced by solar modulation. OULU has been operational since 1964, providing a long-term, high-quality dataset with minimal missing values. This extensive coverage makes it well suited for investigating the long-term variability of cosmic ray intensities and their connection to solar processes.

Sunspot data were obtained from the World Data Center SILSO, Royal Observatory of Belgium, Brussels (`https://www.sidc.be/SILSO/datafiles`) [40]. SILSO provides a continuous, long-term record of sunspot numbers. In this study, we used data that ranged from 1964 to 2024, capturing multiple solar cycles. Since each cycle lasts about 11 years, this time frame includes periods of both solar maxima and minima, thus encompassing a wide range of solar activity conditions.

The sunspot data are recorded with a daily resolution, the finest available for this dataset, allowing for detailed analysis of short-term fluctuations in solar activity and their potential correlation with cosmic ray intensity. For this study, we selected the OULU neutron monitor data due to its completeness and minimal missing values. Any missing values were addressed using a Moving Average Exponentially Weighted procedure, ensuring the integrity of the dataset. No additional data mining or manipulation techniques were applied to the datasets. Both time series (cosmic ray and sunspot data) were normalized using a standard convention to facilitate comparison. The normalization was performed using the formula:

$$\mathrm{data}_{norm} = \frac{\mathrm{data} - \min(\mathrm{data})}{\max(\mathrm{data}) - \min(\mathrm{data})}. \tag{7}$$

This normalization ensures that all time series are on the same scale, enabling more accurate cross-correlation analysis. The datasets encompass multiple solar cycles, with each cycle characterized by varying levels of solar activity and corresponding changes in cosmic ray intensity. The comprehensive span of the data allows for a robust analysis of long-term trends and correlations.

As illustrated in Figure 1(Left), the normalized counts of cosmic rays measured at the OULU station and sunspot numbers from 1964 to 2024 highlight the variability and correlation across multiple solar cycles. The normalization to a [0, 1] scale enables a clear comparison between the two datasets, revealing distinct patterns of variation. The blue line represents the cosmic ray counts, which show significant fluctuations corresponding to solar activity changes, while the orange line shows the sunspot numbers with evident cyclical peaks and troughs. This comparison underscores the inverse relationship between cosmic ray intensity and solar activity, with higher sunspot numbers typically associated with reduced cosmic ray counts due to increased solar activity. The variability observed in both time series is crucial for understanding the dynamic interactions between cosmic rays and solar activity.

Figure 1(Right) provides a detailed scatter plot of cosmic ray counts against sunspot numbers, further emphasizing this inverse relationship. The variability in both time series is apparent, with the cosmic ray intensity decreasing as the sunspot numbers increase. This detailed visualization highlights the importance of considering multifractal properties when analyzing the cross-correlations between these non-stationary time series.

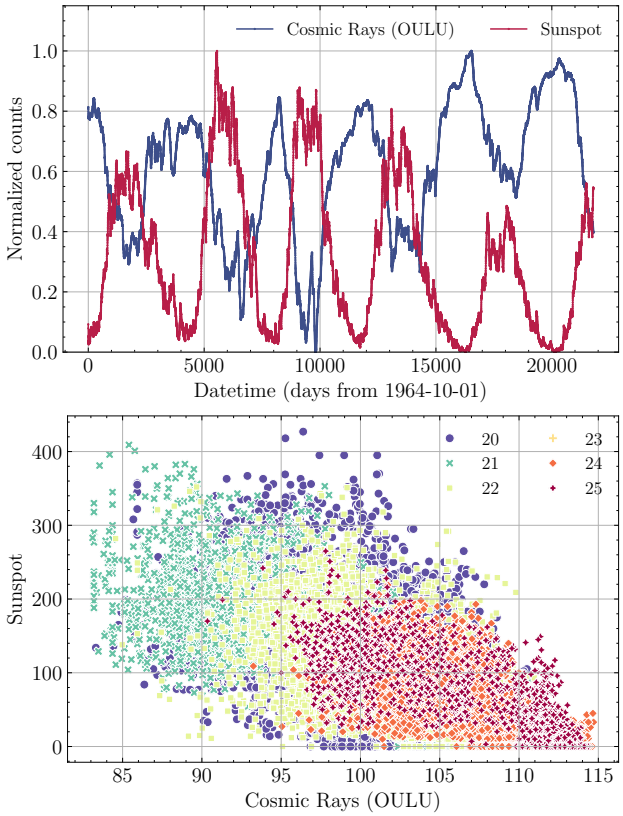

Figure 1: (Left) Normalized counts of cosmic rays (OULU) and sunspots from 1964 to 2024. The data have been normalized to a [0, 1] scale to facilitate comparison. The OULU cosmic ray counts (blue line) and sunspot numbers (red line) are shown, highlighting the variability and correlation patterns over multiple solar cycles. The normalization was performed using the formula 7. (Right) Scatter plot for one-to-one counts (not normalized) between cosmic rays and sunspots showing an evident anti-correlation relationship, with colors referring to the solar cycles across the study. This allows for a direct visual comparison of the two time series.

3. Experimental results

Following the proposed methodology, the first step involved calculating the multifractal cross-correlation coefficient. According to Eq (2), the analysis was performed by dividing each time series into 7 windows of varying window lengths $n = [49, 98, 194, 385, 764, 1515, 3003, 5953]$ (days) logarithmically spaced. These window lengths correspond to minimum and maximum window sizes of approximately 0.25% and 18% of the total data length, respectively, and are spaced linearly. The largest window size, approximately 3900 days, was chosen to coincide with the average length of a solar cycle, capturing long-term phenomena. The smallest window size, 50 days, was selected to include short-term events and fluctuations.

To explore the multifractal nature of the data, we considered fluctuation orders $q = [0.5, 1, 2, 3, 4, 5]$. For the fitting within each window, we employed polynomial functions of orders 2, 3, 4, and 5. The cumulative fluctuation functions in the window sizes were then constructed in accordance with equations (3), (4) and (5) from our methodology.

Figure 2 illustrates the logarithmic plot of the fluctuation functions $F^2_{\mathrm{MFDCCA},xy}$, $F^2_{\mathrm{MFDFA},x}$ and $F^2_{\mathrm{MFDFA},y}$, as a function of window size ($\log n$). These functions were calculated for the joint series (cosmic rays and sunspots) and the individual series (cosmic rays and sunspots), respectively.

From the left panel, depicting $F^2_{\mathrm{MFDCCA},xy}$, we observe that the fluctuation function scales with the window size n following a power law relationship $F^2_{\mathrm{MFDCCA},xy} \sim n^{k_{xy}}$. For $q = 2$, the fitted power law for this function yields an exponent $k_{xy} = 1.775 \pm 0.034$, indicating strong multifractal cross-correlations between the cosmic ray and sunspot series. Similarly, the middle panel shows $F^2_{\mathrm{MFDFA},x}$ for the cosmic ray series, which also follows a power law with an exponent $k_x = 1.827 \pm 0.024$ (for $q = 2$). This exponent reflects the scaling properties and multifractal nature of the

cosmic ray intensity over different time scales. Finally, the right panel presents $F^2_{\mathrm{MFDFA},y}$ for the sunspot series. The power-law fit for this fluctuation function results in an exponent $k_y = 1.675 \pm 0.050$ (for $q = 2$). The slightly higher value of k_y compared to k_x suggests that the sunspot series exhibits stronger multifractal behavior than the cosmic ray series.

Overall, these results indicate that both individual series and their joint behavior display significant multifractality, with consistent scaling properties across different fluctuation orders. The close agreement of the exponents underscores the strong relationship between solar activity and cosmic ray intensity, highlighting the effectiveness of the multifractal detrended cross-correlation analysis in capturing these complex dynamics.

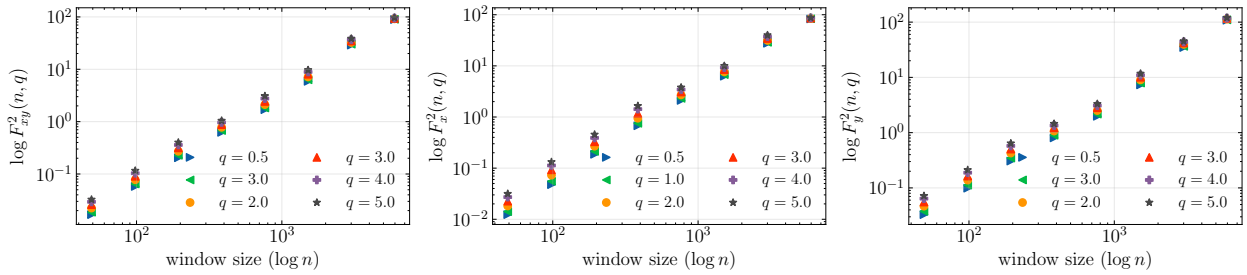

Figure 2: Logarithmic plots of the fluctuation functions $\log F^2_{\mathrm{MFDFA},xy}$ (left), $\log F^2_{\mathrm{MFDFA},x}$ (middle), and $\log F^2_{\mathrm{MFDFA},y}$ (right) as a function of window size $\log n$. The data points correspond to different fluctuation orders $q = [0.5, 1, 2, 3, 4, 5]$. The fitted power law $F^2_{\mathrm{MFDFA},a} \sim n^{k_a}$ exponents are $k_{xy} = 1.775 \pm 0.034$, $k_x = 1.827 \pm 0.024$, and $k_y = 1.675 \pm 0.050$ (for $q = 2$), indicating significant multifractal behavior in both individual and joint series.

Figure 3 presents the multifractal cross-correlation coefficients, $\rho_{\mathrm{MFDCCA}}(n, q)$, calculated for the combined cosmic ray and sunspot time series as a function of the window size n. These coefficients were determined using equation (6) for various polynomial fitting orders (2, 3, 4, and 5) and fluctuation orders $q = [0.5, 1, 2, 3, 4, 5]$.

For polynomial order 2 (top-left panel), the cross-correlation coefficient shows a clear increase trend with window size n. For small window sizes ($n \leq 600$), the coefficients range from 0.75 to 0.85 across different q values. As the window size increases, the coefficients converge towards values between 0.85 and 0.95, indicating stronger correlations at larger scales. The variation across different q values is relatively small, with higher q generally yielding slightly higher coefficients.

Similar behavior is observed in the other panels. For polynomial order 3 (top right panel), there is again a pronounced increasing trend with window size. For small windows, the coefficients range from 0.70 to 0.85, showing more variability than in the polynomial order 2 case. However, for $n \geq 2250$, the coefficients stabilize between 0.85 and 0.95. Differences among q values become more noticeable for medium window sizes (600 to 1700), where higher q values tend to yield higher coefficients.

In the case of polynomial order 4 (bottom-left panel), the trend of increasing cross-correlation coefficients with window size is also evident. For small windows, the coefficients vary from 0.70 to 0.85 with noticeable differences across q values. As n increases, the coefficients stabilize, typically between 0.80 and 0.90, and show less variation. Higher polynomial orders appear to capture more subtle trends, resulting in more consistent coefficients across different q values.

The fluctuation order q also influences these trends. For lower q values (0.5 and 1.0), the coefficients initially show more variability for smaller window sizes, but eventually stabilize and converge to higher values as n increases, regardless of the polynomial order. Intermediate fluctuation orders (2.0 and 3.0) show relatively stable coefficients across window sizes, with coefficients increasing as n increases. Higher fluctuation orders (4.0 and 5.0) consistently yield the highest coefficients, especially at larger window sizes, and show reduced variability, indicating that larger-scale fluctuations in the data are more strongly correlated.

In general, the analysis reveals that the multifractal cross-correlation coefficient $\rho_{\mathrm{MFDCCA}}(n, q)$ increases with window size, reflecting stronger correlations at larger temporal scales. Higher polynomial fitting orders (4 and 5) provide more stable and typically higher coefficients, while the fluctuation order q modulates how strongly certain scales and magnitudes of fluctuations contribute to the correlations.

The trends observed in Figure 3 reflect how the underlying multifractal cross-correlations between cosmic ray

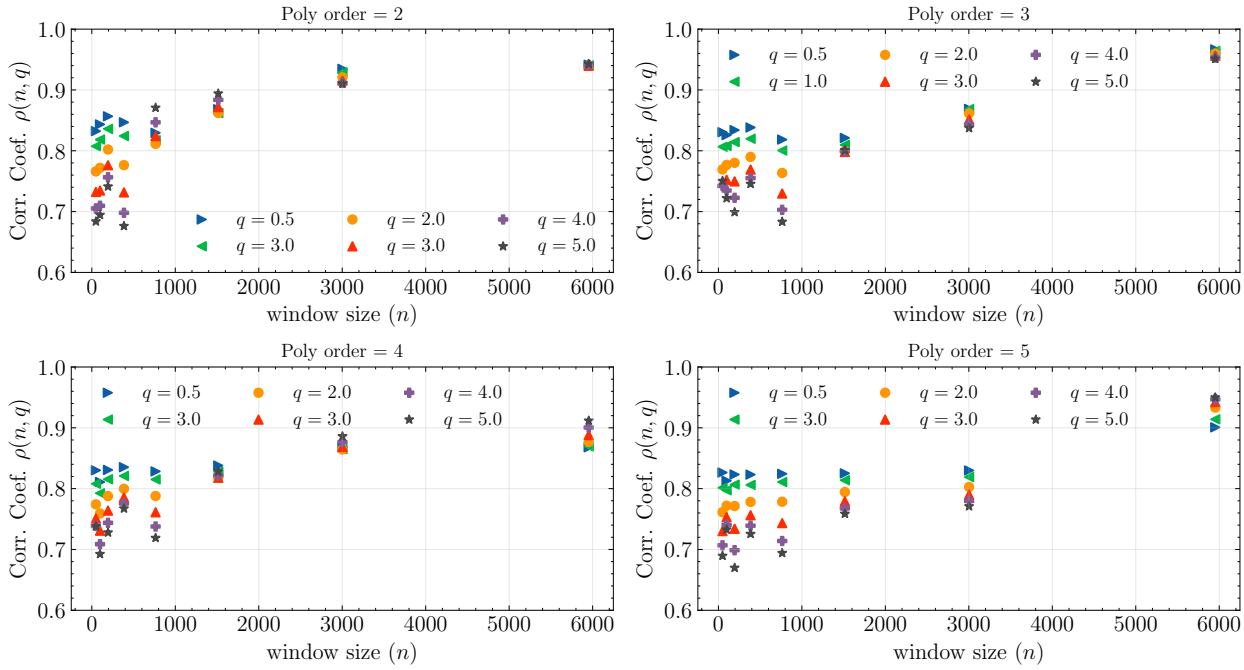

Figure 3: Multifractal cross-correlation coefficients $\rho_{\text{MFDCCA}}(n, q)$ are shown as a function of window size n for different polynomial fitting orders (2, 3, 4, and 5) and fluctuation orders $q = [0.5, 1, 2, 3, 4, 5]$. The coefficients increase with window size, indicating stronger correlations at larger scales. Higher polynomial orders yield more stable and higher coefficients across all window sizes, while higher fluctuation orders q generally result in stronger correlations.

intensity and sunspot numbers vary with both the scale (window size) and the way fluctuations are weighted (via q) and detrended (via polynomial order). Larger window sizes generally reveal stronger long-range correlations, suggesting that at broader temporal scales, the interaction between cosmic ray fluxes and solar activity becomes more pronounced.

The fluctuation order q controls the emphasis placed on different types of fluctuations: lower q-values (e.g., $q = 0.5$) highlight smaller, more subtle fluctuations. The fact that, for $q = 0.5$, the correlation coefficients remain stable and nearly unchanged for higher polynomial orders (4 and 5) indicates that the smaller-scale relationships between the two time series are robust and less sensitive to how the underlying trend is removed. In other words, when focusing on minute variations, a higher polynomial detrending order provides a more consistent baseline, resulting in stable correlation values across different scales.

Physically, these stable correlations at lower q suggest that certain small-scale processes linking cosmic ray intensity and solar activity are persistent and not significantly affected by the choice of polynomial order or the time window considered. At higher q-values, where larger fluctuations carry more weight, the correlation patterns become more sensitive to scale, revealing the complexity and multifractality of the processes involved. This interplay between scale, fluctuation magnitude, and detrending order highlights the multifaceted nature of solar-terrestrial interactions and underscores the importance of carefully selecting parameters when analyzing multifractal correlations in space weather time series.

For the lower polynomial order (e.g., order 2), the dynamic range of the correlation coefficient as a function of window size is relatively limited, making it appear less sensitive to changes in scale. Although no additional resampling or bootstrapping analyses were performed to quantify uncertainties in detail, previous work and standard approaches indicate that the typical uncertainties for correlation coefficients derived from large datasets and stable detrending conditions are generally small. While these uncertainties are not explicitly shown here, their expected magnitude would not significantly alter the observed qualitative trends.

The increasing dynamic range of the correlation coefficients when employing higher polynomial orders carries physical significance. As more complex trends are removed, subtle, scale-dependent correlation structures emerge

more clearly. This suggests that the processes linking cosmic ray intensities and solar activity are inherently multifractal and become more apparent when simpler, lower-order trends are no longer overshadowing them. In this way, the enhanced dynamic range at higher polynomial orders underscores the multifaceted nature of solar-terrestrial interactions and supports the utility of multifractal detrending techniques for uncovering rich, scale-dependent behavior in space weather data.

Figure 4 presents the behavior of the cross-correlation coefficients $\rho_{\mathrm{MFDCCA}}(Lag, q)$ for different time lags (in days) ranging from -250 to 250. The four panels correspond to polynomial fitting orders of 2, 3, 4, and 5, respectively, while the different curves in each panel represent various fluctuation orders (q).

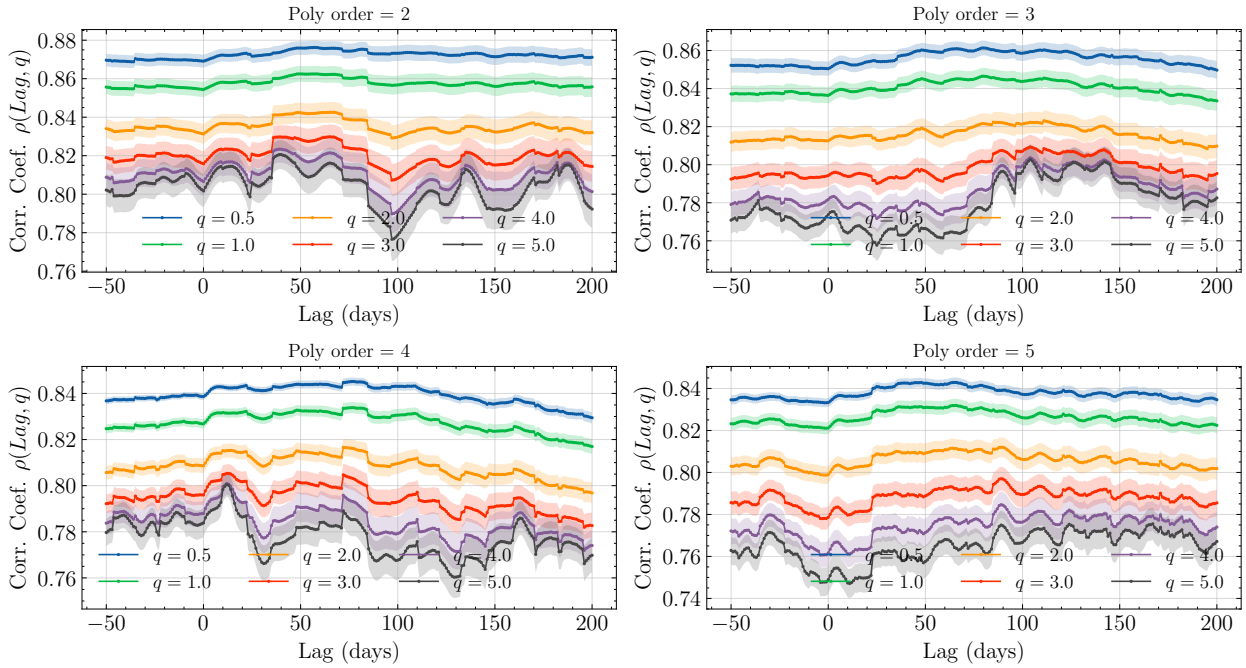

Figure 4: Multifractal cross-correlation coefficients $\rho_{\mathrm{MFDCCA}}(Lag, q)$ as a function of time lag (days) for different polynomial fitting orders (2, 3, 4, and 5) and fluctuation orders q. The coefficients exhibit significant variability with time lag, showing distinct peaks where the correlation is maximized. The lag at which the maximum correlation occurs provides insight into the time delay between cosmic ray intensity and sunspot numbers.

Across all panels, the cross-correlation coefficients exhibit noticeable variability with time lag, showing distinct peaks where the correlation is maximized. For polynomial order 2, the highest correlation occurs for q=0.5 at a lag of 137 days, reaching approximately 0.904. The fluctuations in the correlation coefficients around the peak suggest a typical uncertainty of approximately ±0.005, as inferred from the variations in the surrounding flat regions. Compared to the dynamic range of the coefficients, which spans from about 0.86 in the flatter regions to 0.904 at the peak, this level of uncertainty is small and does not significantly impact the interpretation of the observed trends.

For polynomial order 3, the maximum correlation for $q = 0.5$ occurs at a lag of 80 days with a coefficient of about 0.861. The correlation coefficients for other q values peak at varying lags, with $q = 5.0$ reaching its maximum at a lag of 104 days with a coefficient of 0.802. In the case of polynomial order 4, the maximum correlation for $q = 0.5$ is observed at a lag of 77 days with a coefficient of approximately 0.845. The correlation coefficients gradually decrease as q increases, with higher q-values (e.g., q=3.0,4.0,5.0) peaking at a lag of 12 days with coefficients close to 0.800.

For polynomial order 5, the highest correlation for $q = 0.5$ is found at a lag of 65 days with a coefficient of around 0.842. The correlation coefficients for other q values show slightly different behavior, with $q = 5.0$ exhibiting its peak correlation at a longer lag of 167 days and a reduced coefficient of 0.775.

These observations highlight the variability in cross-correlation coefficients across different time lags, polynomial orders, and fluctuation orders. The lag at which the maximum correlation occurs provides insight into the time delay between cosmic ray intensity and sunspot numbers. The updated summary of the maximum correlation values and

their corresponding lag times is presented in Table 1.

Table 1: Summary of maximum correlation coefficients and corresponding lag times for different fluctuation orders and polynomial fitting orders.

q	Poly. Order	Lag (days)	Max Corr. Coef.
0.5	2	57	0.876
1.0	2	50	0.862
2.0	2	67	0.842
3.0	2	65	0.829
4.0	2	39	0.823
5.0	2	40	0.820
0.5	3	80	0.861
1.0	3	80	0.84
2.0	3	111	0.823
3.0	3	104	0.809
4.0	3	104	0.803
5.0	3	104	0.802
0.5	4	77	0.845
1.0	4	77	0.833
2.0	4	72	0.816
3.0	4	12	0.805
4.0	4	12	0.800
5.0	4	12	0.800
0.5	5	65	0.842
1.0	5	66	0.831
2.0	5	89	0.811
3.0	5	89	0.797
4.0	5	89	0.784
5.0	5	167	0.775

4. Discussion and conclusions

The results of our multifractal cross-correlation analysis reveal significant insights into the dynamic relationship between cosmic ray intensity and sunspot numbers. Our findings indicate strong multifractal correlations across different time scales, with varying degrees of correlation depending on the polynomial order and fluctuation order used in the analysis.

These results are consistent with previous studies that have examined the correlation and time lag between cosmic ray intensity and solar activity. For instance, [27, 41] observed notable time lags between solar activity and galactic cosmic ray intensity, with the correlation peaking at different lags depending on the solar cycle phase. Similarly, [42] (also [43, 27]) found significant time delays between cosmic ray flux and solar activity indicators using wavelet analysis and cross-correlation methods. Our findings, showing maximum correlations at lags ranging from 5 to 192 days, align well with these studies, indicating the robustness of our multifractal approach in capturing these complex dynamics.

The highest correlation coefficients observed in our study, particularly for $q = 0.5$ and polynomial order 2, suggest that the interaction between cosmic rays and solar activity is strongest at specific lag times. These results corroborate the findings of [26], who reported strong cross-correlations between solar wind parameters and cosmic ray intensity, highlighting the multifaceted nature of these interactions over different time scales.

Moreover, our analysis extends the traditional DCCA by incorporating multifractal properties, providing a more nuanced understanding of the time-dependent correlations between these two critical time series. The consistent and robust results across different polynomial and fluctuation orders underscore the efficacy of the MFDCCA in elucidating the underlying relationships in non-stationary data.

Our study contributes to the growing body of literature that seeks to understand the intricate connections between solar activity and cosmic ray intensity. The observed time lags and correlation coefficients are in good agreement with previous research, reinforcing the significance of multifractal analysis in space weather studies. Future work could further explore these relationships by incorporating additional datasets and refining the analytical techniques to provide even deeper insights into the multifractal nature of these complex interactions.

Our findings underscore the importance of utilizing advanced techniques beyond traditional correlation methods for analyzing the relationship between cosmic ray intensity and sunspot numbers. Traditional correlation techniques often fail to capture the multifractal nature and variability of these time series on different time scales. By employing Multifractal Detrended Cross-Correlation Analysis (MFDCCA), we have better characterized the complex and multifaceted interactions between these two phenomena. This approach allows for a more nuanced understanding of the varying degrees of correlation at different scales, revealing insights that would be overlooked using simpler methods. The ability of MFDCCA to account for multifractality is particularly crucial given the non-stationary and heterogeneous nature of cosmic ray and solar activity data, which exhibit distinct behaviors over short and long time scales.

Furthermore, we recommend extending this study by incorporating additional heliophysical variables and measurements. Including parameters such as solar wind conditions, the interplanetary magnetic field, coronal mass ejection (CME) indices, and flare indices would provide a more comprehensive view of the influences on cosmic ray intensity. These variables play significant roles in modulating cosmic rays and could enhance our understanding of the underlying mechanisms driving their variability. By integrating these additional datasets, future studies could develop a more robust multifractal model that captures the intricate interactions between cosmic rays and a broader range of solar and heliospheric phenomena. This holistic approach would not only validate our current findings but also pave the way for more accurate predictions and deeper insights into space weather dynamics.

In this study, the multifractal cross-correlation coefficient $\rho_{MFDCCA}(n,q)$ was calculated using a definition that considers the magnitude of the fluctuations, resulting in values ranging between 0 and 1. While this approach effectively highlights the strength of the correlations, future work may consider implementing an alternative definition that retains the sign of the fluctuations. This would allow the coefficient to range between -1 and 1, capturing both the direction and magnitude of the correlation. Given the well-established negative relationship between cosmic ray intensity and sunspot numbers, incorporating the sign would provide a more complete characterization of the underlying interactions. Such refinements could further enhance the interpretability and applicability of multifractal analyses in space weather research.

acknowledgements

The authors would like to thank the UTB Research Department for its unconditional support in this research. While the research has not been funded by any institution or entity, the author is grateful to UTB for the computer equipment provided for the development of the research activity and the generation of scientific computing results.

We gratefully acknowledge the data providers whose contributions have made this research possible. The cosmic ray data were obtained from the Neutron Monitor Data Base (NMDB, `https://www.nmdb.eu/`), with special thanks to the OULU station for their high-quality and continuous measurements. We also extend our appreciation to the World Data Center SILSO, Royal Observatory of Belgium, Brussels (`https://www.sidc.be/SILSO/datafiles`), for supplying the sunspot number data. These invaluable datasets have been fundamental to our analysis and have greatly facilitated the advancement of our understanding of the complex interactions between cosmic ray intensity and solar activity.

References

[1] L. Del Rio Amador, S. Lovejoy, Long-range forecasting as a past value problem: Untangling correlations and causality with scaling, Geophysical Research Letters 48 (9) (2021) e2020GL092147. doi:https://doi.org/10.1029/2020GL092147.

[2] L. Kristoufek, Multifractal height cross-correlation analysis: A new method for analyzing long-range cross-correlations, Europhysics Letters 95 (6) (2011) 68001. doi:https://doi.org/10.1209/0295-5075/95/68001.

[3] S. Arianos, A. Carbone, Cross-correlation of long-range correlated series, Journal of Statistical Mechanics: Theory and Experiment 2009 (03) (2009) P03037. doi:https://doi.org/10.1088/1742-5468/2009/03/P03037.

[4] B. Podobnik, H. E. Stanley, Detrended cross-correlation analysis: A new method for analyzing two nonstationary time series, Physical Review Letters 100 (8) (2008) 084102. doi:https://doi.org/10.1103/PhysRevLett.100.084102.
[5] D. Horvatic, H. E. Stanley, B. Podobnik, Detrended cross-correlation analysis for non-stationary time series with periodic trends, Europhysics Letters 94 (1) (2011) 18007. doi:https://doi.org/10.1209/0295-5075/94/18007.
[6] F. Wang, J. Xu, Q. Fan, Statistical properties of the detrended multiple cross-correlation coefficient, Communications in Nonlinear Science and Numerical Simulation 99 (2021) 105781. doi:https://doi.org/10.1016/j.cnsns.2021.105781.
[7] G. F. Zebende, Dcca cross-correlation coefficient: Quantifying level of cross-correlation, Physica A: Statistical Mechanics and its Applications 390 (4) (2011) 614–618. doi:https://doi.org/10.1016/j.physa.2010.10.022.
[8] G. Zebende, A. da Silva Filho, Detrended multiple cross-correlation coefficient, Physica A: Statistical Mechanics and its Applications 510 (2018) 91–97. doi:https://doi.org/10.1016/j.physa.2018.06.119.
[9] B. Podobnik, Z.-Q. Jiang, W.-X. Zhou, H. E. Stanley, Statistical tests for power-law cross-correlated processes, Physical Review E 84 (6) (2011) 066118. doi:https://doi.org/10.1103/PhysRevE.84.066118.
[10] P. Ma, D. Li, S. Li, Efficiency and cross-correlation in equity market during global financial crisis: Evidence from china, Physica A: Statistical Mechanics and Its Applications 444 (2016) 163–176. doi:https://doi.org/10.1016/j.physa.2015.10.019.
[11] M. Wkatorek, S. Drożdż, J. Kwapień, L. Minati, P. Oświkecimka, M. Stanuszek, Multiscale characteristics of the emerging global cryptocurrency market, Physics Reports 901 (2021) 1–82. doi:https://doi.org/10.1016/j.physrep.2020.10.005.
[12] S. Drożdż, J. Kwapień, P. Oświkecimka, T. Stanisz, M. Wkatorek, Complexity in economic and social systems: Cryptocurrency market at around covid-19, Entropy 22 (9) (2020) 1043. doi:https://doi.org/10.3390/e22091043.
[13] G. Cao, C. He, W. Xu, Effect of weather on agricultural futures markets on the basis of dcca cross-correlation coefficient analysis, Fluctuation and Noise Letters 15 (02) (2016) 1650012. doi:https://doi.org/10.1142/S0219477516500127.
[14] C.-h. Shen, C.-l. Li, Y.-l. Si, A detrended cross-correlation analysis of meteorological and api data in nanjing, china, Physica A: Statistical Mechanics and its Applications 419 (2015) 417–428. doi:https://doi.org/10.1016/j.physa.2014.10.058.
[15] H. Tatli, Ş. S. Menteş, Detrended cross-correlation patterns between north atlantic oscillation and precipitation, Theoretical and Applied Climatology 138 (1) (2019) 387–397. doi:https://doi.org/10.1007/s00704-019-02827-7.
[16] C. Zhang, Z. Ni, L. Ni, Multifractal detrended cross-correlation analysis between pm2. 5 and meteorological factors, Physica A: Statistical Mechanics and its Applications 438 (2015) 114–123. doi:https://doi.org/10.1016/j.physa.2015.06.039.
[17] W. Xu, C. Liu, K. Shi, Y. Liu, Multifractal detrended cross-correlation analysis on no, no2 and o3 concentrations at traffic sites, Physica A: Statistical Mechanics and its Applications 502 (2018) 605–612. doi:https://doi.org/10.1016/j.physa.2018.02.114.
[18] C. Varotsos, G. Golitsyn, M. Efstathiou, N. Sarlis, A new method of nowcasting extreme cosmic ray events, Remote Sensing Letters 14 (6) (2023) 576–584. doi:https://doi.org/10.1080/2150704X.2022.2057204.
[19] C. Varotsos, G. Golitsyn, Y. Xue, M. Efstathiou, N. Sarlis, T. Voronova, On the relation between rain, clouds, and cosmic rays, Remote Sensing Letters 14 (3) (2023) 301–312. doi:https://doi.org/10.1080/2150704X.2023.2190468.
[20] J. Christodoulakis, C. Varotsos, H. Mavromichalaki, M. Efstathiou, M. Gerontidou, On the link between atmospheric cloud parameters and cosmic rays, Journal of Atmospheric and Solar-Terrestrial Physics 189 (2019) 98–106. doi:https://doi.org/10.1016/j.jastp.2019.04.012.
[21] S. Gopinath, P. Prince, Multifractal characteristics of magnetospheric dynamics and their relationship with sunspot cycle, Advances in Space Research 59 (9) (2017) 2265–2278. doi:https://doi.org/10.1016/j.asr.2017.02.011.
[22] D. Sierra-Porta, A multifractal approach to understanding forbush decrease events: Correlations with geomagnetic storms and space weather phenomena, Chaos, Solitons & Fractals 185 (2024) 115089. doi:https://doi.org/10.1016/j.chaos.2024.115089.
[23] D. Sierra-Porta, A.-R. Domínguez-Monterroza, Linking cosmic ray intensities to cutoff rigidity through multifractal detrented fluctuation analysis, Physica A: Statistical Mechanics and its Applications 607 (2022) 128159. doi:https://doi.org/10.1016/j.physa.2022.128159.
[24] D. Sierra-Porta, Relationship between magnetic rigidity cutoff and chaotic behavior in cosmic ray time series using visibility graph and network analysis techniques, Chaos: An Interdisciplinary Journal of Nonlinear Science 34 (2) (2024). doi:https://doi.org/10.1063/5.0167156.
[25] D. Sierra-Porta, On the fractal properties of cosmic rays and sun dynamics cross-correlations, Astrophysics and Space Science 367 (12) (2022) 116. doi:https://doi.org/10.1007/s10509-022-04151-5.
[26] K. Iskra, M. Siluszyk, M. Alania, W. Wozniak, Experimental investigation of the delay time in galactic cosmic ray flux in different epochs of solar magnetic cycles: 1959–2014, Solar Physics 294 (9) (2019) 115. doi:https://doi.org/10.1007/s11207-019-1509-4.
[27] D. Sierra-Porta, Cross correlation and time-lag between cosmic ray intensity and solar activity during solar cycles 21, 22 and 23, Astrophysics and Space Science 363 (2018) 1–5. doi:https://doi.org/10.1007/s10509-018-3360-8.
[28] J. Takalo, Extracting hale cycle related components from cosmic-ray data using principal component analysis, Solar Physics 297 (9) (2022) 113. doi:https://doi.org/10.1007/s11207-022-02048-8.
[29] S. A. Koldobskiy, R. Kähkönen, B. Hofer, N. A. Krivova, G. A. Kovaltsov, I. G. Usoskin, Time lag between cosmic-ray and solar variability: Sunspot numbers and open solar magnetic flux, Solar Physics 297 (3) (2022) 38. doi:https://doi.org/10.1007/s11207-022-01970-1.
[30] C. Idosa, A. Giri, B. Adhikari, E. Mosisa, C. Gashu, Variations of cosmic ray intensity with the solar flare index, coronal index, and geomagnetic indices: Wavelet and cross correlation approaches, Physics of Plasmas 30 (8) (2023). doi:https://doi.org/10.1063/5.0157553.
[31] R. Modzelewska, A. Krasińska, A. Wawrzaszek, A. Gil, Scaling features of diurnal variation of galactic cosmic rays, Solar Physics 296 (8) (2021) 125. doi:https://doi.org/10.1007/s11207-021-01866-6.
[32] J. Kwapień, P. Oświkecimka, S. Drożdż, Detrended fluctuation analysis made flexible to detect range of cross-correlated fluctuations, Physical Review E 92 (5) (2015) 052815. doi:https://doi.org/10.1103/PhysRevE.92.052815.
[33] G. Rice, M. Shum, Inference for the lagged cross-covariance operator between functional time series, Journal of Time Series Analysis 40 (5) (2019) 665–692. doi:https://doi.org/10.1111/jtsa.12447.
[34] M. L. O. Salvana, M. G. Genton, Nonstationary cross-covariance functions for multivariate spatio-temporal random fields, Spatial Statistics

37 (2020) 100411. doi:https://doi.org/10.1016/j.spasta.2020.100411.
[35] L. R. Gorjao, G. Hassan, J. Kurths, D. Witthaut, Mfdfa: Efficient multifractal detrended fluctuation analysis in python, Computer Physics Communications 273 (2022) 108254. doi:https://doi.org/10.1016/j.cpc.2021.108254.
[36] X. Zhang, G. Zhang, L. Qiu, B. Zhang, Y. Sun, Z. Gui, Q. Zhang, A modified multifractal detrended fluctuation analysis (mfdfa) approach for multifractal analysis of precipitation in dongting lake basin, china, Water 11 (5) (2019) 891. doi:https://doi.org/10.3390/w11050891.
[37] H. Mavromichalaki, A. Papaioannou, C. Sarlanis, G. Souvatzoglou, M. Gerontidou, C. Plainaki, M. Papailiou, G. Mariatos, N. Team, Establishing and using the real-time neutron monitor database (nmdb), in: 9th International Conference of the Hellenic Astronomical Society, Vol. 424, 2010, p. 75.
[38] D. Sapundjiev, T. Verhulst, S. Stankov, International database of neutron monitor measurements: Development and applications, in: Knowledge Discovery in Big Data from Astronomy and Earth Observation, Elsevier, 2020, pp. 371–383. doi:https://doi.org/10.1016/B978-0-12-819154-5.00032-1.
[39] C. Steigies, N. Fuller, et al., Accessing nmdb data using nest and pandas, in: NMDB@ Athens: Proceedings of the hybrid symposium on cosmic ray studies with neutron detectors, September 26-30, 2022, 2023, pp. 211–217. doi:https://doi.org/10.38072/2748-3150/p44.
[40] SILSO World Data Center, The international sunspot number, International Sunspot Number Monthly Bulletin and online catalogue (1964-2024).
[41] D. Sierra-Porta, Revised cross-correlation and time-lag between cosmic ray intensity and solar activity using chatterjee's correlation coefficient, Advances in Space Research 75 (1) (2024). doi:https://doi.org/10.1016/j.asr.2024.10.065.
URL https://www.sciencedirect.com/science/article/pii/S0273117724010974
[42] K. Kudela, J. Rybák, A. Antalová, M. Storini, Time evolution of low-frequency periodicities in cosmic ray intensity, Solar Physics 205 (1) (2002) 165–175. doi:https://doi.org/10.1023/A:1013869322693.
[43] P. Chowdhury, K. Kudela, Quasi-periodicities in cosmic rays and time lag with the solar activity at a middle latitude neutron monitor: 1982–2017, Astrophysics and Space Science 363 (2018) 1–17. doi:https://doi.org/10.1007/s10509-018-3467-y.